Safe and Efficient Gene Therapy for Pyruvate Kinase Deficiency

Maria Garcia-Gomez[1,2], Andrea Calabria[3], Maria Garcia-Bravo[1,2], Fabrizio Benedicenti[3], Penelope Kosinski[4], Sergio López-Manzaneda[1,2], Collin Hill[4], María del Mar Mañu-Pereira[5], Miguel A Martín[1,2], Israel Orman[1,2], Joan-LLuis Vives-Corrons[5], Charles Kung[4], Axel Schambach[6], Shengfang Jin[4], Juan A Bueren[1,2], Eugenio Montini[3], Susana Navarro[1,2] and Jose C Segovia[1,2]

[1]Hematopoietic Innovative Therapies Division, Centro de Investigaciones Energéticas, Medioambientales y Tecnológicas (CIEMAT) - Centro de Investigaciones Biomédicas en Red de Enfermedades Raras (CIBERER), Madrid, Spain; [2]Advanced Therapies Mixed Unit. Instituto de Investigación Sanitaria-Fundación Jiménez Díaz (IIS-FJD), Madrid, Spain; [3]San Raffaele Telethon Institute for Gene Therapy (HSR-TIGET), San Raffaele Scientific Institute, Milan, Italy; [4]Agios Pharmaceuticals, Cambridge, MA, USA; [5]Red Cell Pathology Laboratory. Hospital Clínic of Barcelona – Institut d'Investigacions Biomèdiques August Pi i Sunyer, Barcelona, Spain; [6]Institute of Experimental Hematology at Hannover Medical Hospital, Hannover, Germany

Pyruvate kinase deficiency (PKD) is a monogenic metabolic disease caused by mutations in the *PKLR* gene that leads to hemolytic anemia of variable symptomatology and that can be fatal during the neonatal period. PKD recessive inheritance trait and its curative treatment by allogeneic bone marrow transplantation provide an ideal scenario for developing gene therapy approaches. Here, we provide a preclinical gene therapy for PKD based on a lentiviral vector harboring the hPGK eukaryotic promoter that drives the expression of the *PKLR* cDNA. This therapeutic vector was used to transduce mouse PKD hematopoietic stem cells (HSCs) that were subsequently transplanted into myeloablated PKD mice. Ectopic RPK expression normalized the erythroid compartment correcting the hematological phenotype and reverting organ pathology. Metabolomic studies demonstrated functional correction of the glycolytic pathway in RBCs derived from genetically corrected PKD HSCs, with no metabolic disturbances in leukocytes. The analysis of the lentiviral insertion sites in the genome of transplanted hematopoietic cells demonstrated no evidence of genotoxicity in any of the transplanted animals. Overall, our results underscore the therapeutic potential of the hPGK-coRPK lentiviral vector and provide high expectations toward the gene therapy of PKD and other erythroid metabolic genetic disorders.

Received 20 August 2015; accepted 25 March 2016; advance online publication 14 June 2016. doi:10.1038/mt.2016.87

INTRODUCTION

Among many other hereditary enzymatic defects affecting the erythrocytes, pyruvate kinase deficiency (PKD) is the most frequent one causing chronic nonspherocytic hemolytic anemia.[1] Onset and severity of PKD are very variable and range from mild to severe neonatal anemia, becoming fatal during the childhood in the most severe cases.[2] Growth retardation, *hydrops fetalis*, and death during the neonatal period have also been reported with low frequency.[3] PKD prevalence has been estimated at 1:20,000 in the general Caucasian population[4] and, so far, more than 195 different mutations in the *PKLR* gene have been identified (http://www.lovd.nl/pklr). Allogeneic bone marrow transplantation has been successfully used to cure severe PKD patients,[5] but the low availability of histocompatible donors and the serious complications associated with the bone marrow transplantation of these patients (*i.e.*, graft versus host disease, opportunistic infections, etc.) make periodic blood transfusions and splenectomy the main therapeutic options for most of the severe forms of PKD,[6] dramatically increasing patient morbidity and mortality.[7] The limited efficacy and side effects of the therapeutic options for severe PKD patients and its recessive inheritance trait make PKD a suitable disease to be treated by gene therapy.

PKD is caused by defects in the pyruvate kinase (PK) enzyme[6] that catalyzes the last ATP-generating reaction of the glycolysis pathway in all cells. In mature erythrocytes, PK becomes essential as RBCs only express the R-type-specific isoform (RPK)[8] due to the regulation of the erythroid-specific alternative promoter of the *PKLR* locus.[9] Thus, any loss of RPK activity impairs RBC metabolism and lifespan,[6] leading to chronic nonspherocytic hemolytic anemia.

Gene therapy for monogenic diseases, particularly those affecting the hematopoietic system, has provided convincing evidence that genetic correction of autologous hematopoietic stem cells (HSCs) is an alternative therapeutic option to allogeneic HSCT, avoiding its major complications.[10–14] Genetic correction for diseases affecting the erythrocyte such as β-thalassemia and sickle cell disease, have been addressed in animal models[15,16] and also in humans.[11] However, gene therapy approaches for inherited erythroid metabolic deficiencies such as PKD are still limited. The feasibility of HSC gene therapy for PKD has been demonstrated both in mouse[17,18] and in dog RPK-deficient experimental models,[19] showing that donor chimerism and transduction levels are

Correspondence: Jose C Segovia, Hematopoietic Innovative Therapies Division, Centro de Investigaciones Energéticas, Medioambientales y Tecnológicas (CIEMAT) - Centro de Investigaciones Biomédicas en Red de Enfermedades Raras (CIBERER), CIEMAT (Edificio 70), Av. Complutense, 40, 28040 Madrid, Spain. E-mail: jc.segovia@ciemat.es

key points to reach an efficient correction of the hemolytic phenotype[20] given the lack of selective advantage of donor gene-corrected HSCs. Our previous work with a PKD mouse model demonstrated that retrovirally-derived human RPK expression was capable of fully correcting PKD phenotype when over 25% genetically corrected cells were transplanted.[18] A similar therapeutic threshold of corrected cells was recently reported in one PKD Basenji dog infused with foamy vector-corrected and *in vivo* expanded HSCs.[19]

High levels of transgene expression can be achieved when γ-retroviral (γ-RV) vectors are used due to the fact that the therapeutic transgene expression is regulated by their long terminal repeats (LTR) sequences. However, the first clinical trials based on this type of vectors raised safety concerns, as several patients developed unexpected leukemias.[21] The strong promoter activity of LTR sequences could affect the regulation of surrounding genes, either by activation of proto-oncogene promoters or by inhibition of tumor suppressor genes, leading to insertional mutagenesis.[22–25] These findings highlighted the need to use safer and more efficient vectors than γ-retroviral vectors for the PKD gene therapy.

Here, we provide an RPK lentiviral vector (LV) for the genetic correction of PKD. Genetic modification of murine PKD-HSCs with this vector was able to efficiently correct the hemolytic phenotype and the RBC metabolite profile in transplanted PKD mice. Remarkably, no evidence of metabolic disturbances in leukocytes and genotoxicity derived from the vector integration were observed, supporting the therapeutic potential of the PGK-coRPK LV vector. Overall, our preclinical results provide encouraging evidence of the feasibility of gene therapy for PKD with a LV designed for clinical application.

RESULTS

PGK-coRPK therapeutic lentiviral vector leads to a stable and long-term correction of the anemic phenotype in genetically corrected PKD mice

In vivo efficacy of the PGK-coRPK LV (**Supplementary Figure S1a**) was assayed by transduction and transplantation of lineage depleted BM cells (Lin$^-$ cells) from PKD mice (**Supplementary Figure S1b**). Lethally irradiated PKD mice transplanted with deficient cells transduced with the coRPK LV showed a significant improvement in all tested blood erythroid parameters when compared to nontransplanted PKD littermates or to mice transplanted with cells transduced with an enhanced green fluorescent protein (EGFP) LV (**Figure 1** and **Supplementary Table S1**). RBC counts increased as soon as 40 days post-transplantation (**Figure 1a**) and constitutive reticulocytosis, which is one of the most common signs of PKD, was significantly reverted in mice carrying the PGK-coRPK transgene, reaching levels close to those observed in healthy controls for at least 9 months after transplant (**Figure 1b**). On the contrary, PKD animals transplanted with EGFP LV-transduced cells showed anemia and remarkable reticulocytosis in parallel with PKD mice at all time-points analyzed. Hemoglobin levels, hematocrit index, mean corpuscular volume, and mean corpuscular hemoglobin values were also corrected in mice transplanted with lentivirally corrected cells when compared to nontransplanted PKD littermates (**Supplementary Table S1**). This hematological correction was achieved with 63.66 ± 4.45% of donor chimerism and transduction efficacies ranging from 60 to 90% (**Supplementary Table S2**). Transduced cells showed on average 1.65 ± 0.08 integrated vector copies per cell (VCN), indicating that PGK-coRPK LV-vector provided enough human RPK transgenic expression to revert the hemolytic anemia. Remarkably, the expression of the coRPK transgene led to an extension of erythroid cell half-life when compared to nontransplanted PKD mice (**Figure 1c,d**). On average, PKD mice showed a RBC half-life of 19 days, while in genetically corrected mice this was extended to 25 days (6 days' extension) reaching values close to wild-type RBC half-life (**Figure 1d**). Thus, RBCs of coRPK-expressing mice displayed intermediate survival kinetics between healthy and deficient control mice (**Figure 1c**), most likely because full chimerism was not achieved in these animals (**Supplementary Table S2**).

Nine months after transplant hematopoietic progenitors from primary recipients were transplanted into secondary recipients that maintained engraftment levels (62.89 ± 5.61%) and viral copy number (VCN) (1.44 ± 0.08 copies) (**Supplementary Table S2**). Secondary transplanted recipients showed a multi-lineage hematopoietic reconstitution up to 5 months post-transplantation (**Supplementary Figure S2**) and a significant improvement in all PB erythroid parameters (**Figure 2** and **Supplementary Table S1**). In addition, proviral integrations were detected in differently committed hematopoietic progenitors (**Supplementary Figure S3a,b**) and its number remained constant over time (**Supplementary Figure S3c**) demonstrating the stability of the genetic correction and highlighting the safety of the PGK-coRPK LV.

Lentiviral-derived RPK expression normalizes erythroid differentiation and allows the production of functional mature erythrocytes

PKD mice show a characteristic expansion of the erythroid compartment caused by the compensatory erythropoiesis mechanism.[26] The study of the erythroid differentiation pattern in transplanted mice indicated that the ectopic RPK expression reverted this mechanism (**Figure 3a,b**). PKD and EGFP-expressing mice showed a predominance of immature erythroid precursors (subpopulation I: proerythroblasts and subpopulation II: basophilic erythroblasts) in BM and spleen, and a remarkable fall in late erythroid cells (population IV: reticulocytes and mature erythrocytes), while mice transplanted with cells transduced with the coRPK LV showed a significant reduction of immature erythroid precursors (subpopulations I and II) in BM and spleen, and a significant increase of the latest erythroid compartment (subpopulation IV) equivalent to healthy mice (**Figure 3a,b**). In addition, unlike PKD and EGFP-expressing mice, those carrying the coRPK transgene showed a significant reduction of erythropoietin (Epo) levels in plasma (**Figure 3c**). The normalization of the erythropoiesis in PKD mice treated with the therapeutic vector was accompanied by a reduction of the splenic number of progenitors content to normal levels (**Supplementary Figure S4a**), although no changes in the BM colony forming units (CFU) content were noted (**Supplementary Figure S4b**).

Transplantation of cells transduced with the coRPK lentiviral vector reverts extramedullar erythropoiesis and organ pathology

Due to the active destruction of RPK deficient erythrocytes, PKD and EGFP-expressing mice displayed acute splenomegaly with

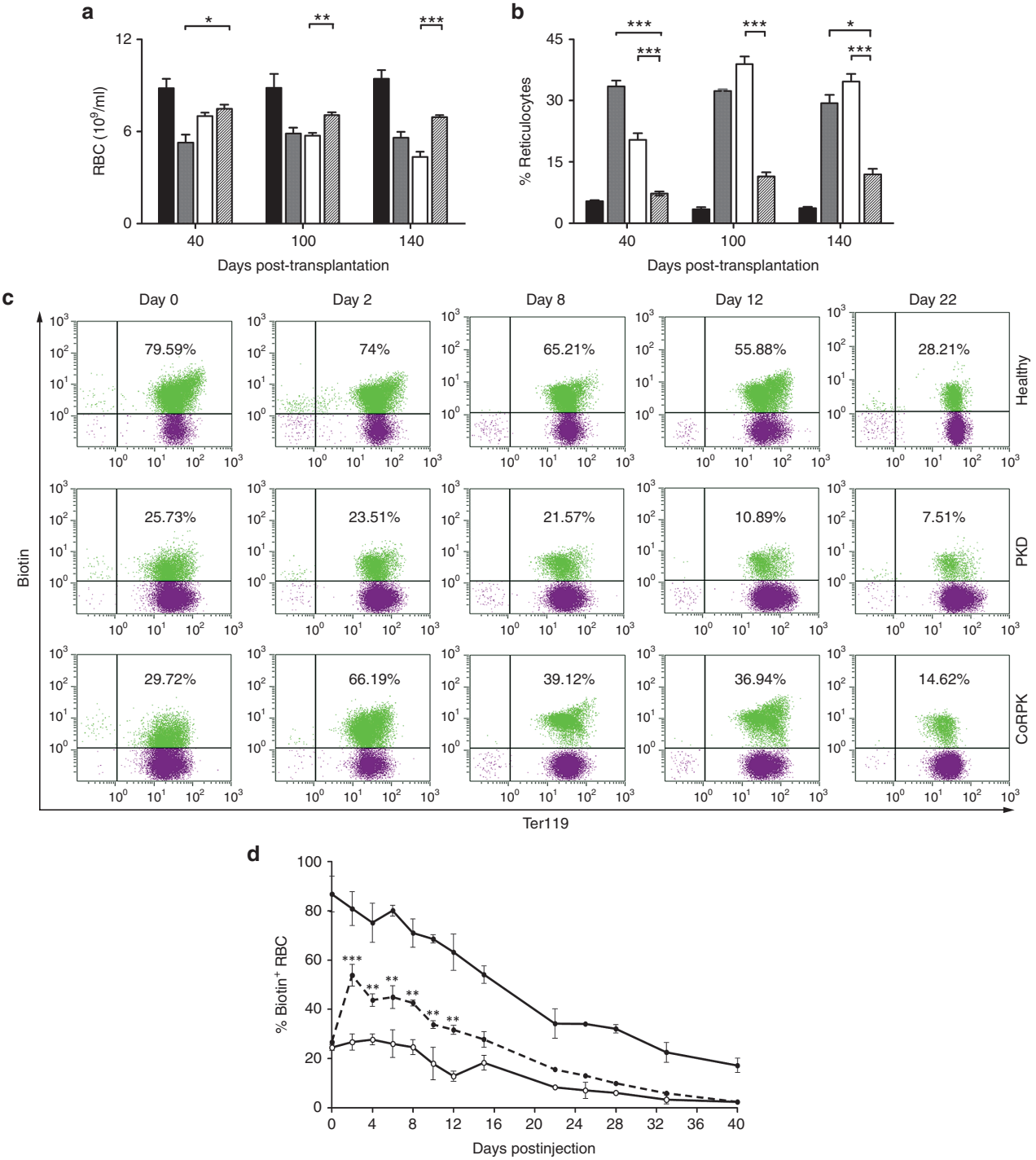

Figure 1 Correction of pyruvate kinase deficiency (PKD) phenotype in peripheral blood of primary recipients after genetic correction. (**a**) RBCs and (**b**) reticulocyte levels in healthy (black bar, $n = 5$) and PKD anemic mice (gray bar, $n = 6$), and PKD anemic mice that were tranplanted with EGFP (white bar, $n = 9$) or coRPK-transduced cells (scratched bar, $n = 17$). Data are represented as the average ± SEM and were analyzed by non-parametric Kruskal-Wallis test. (**c**) Flow cytometry strategy used to detect the biotin-labeled RBCs throughout the time and (**d**) RBC survival kinetics in healthy (black dots, $n = 2$), anemic (white dots, $n = 2$) and genetically corrected mice (discontinuous line, $n = 4$). Data are represented as the average ± standard error of the mean and were analyzed by two-way analysis of variance test. Healthy, nontransplanted control mice; PKD, nontransplanted PKD mice; coRPK, PKD mice expressing the therapeutic transgene.

an increase of spleen weight and size of over 200% when compared to healthy controls (Figure 4a,b). A disorganized structure of the splenic tissue and the expansion of the spleen red pulp were also observed in these animals, indicating an intense extramedullar erythropoiesis also supported by the presence of erythroid cell clusters in PKD and EGFP-expressing liver sections (Figure 4c). Remarkably, the ectopic expression of coRPK transgene completely reverted spleen and liver pathology in genetically

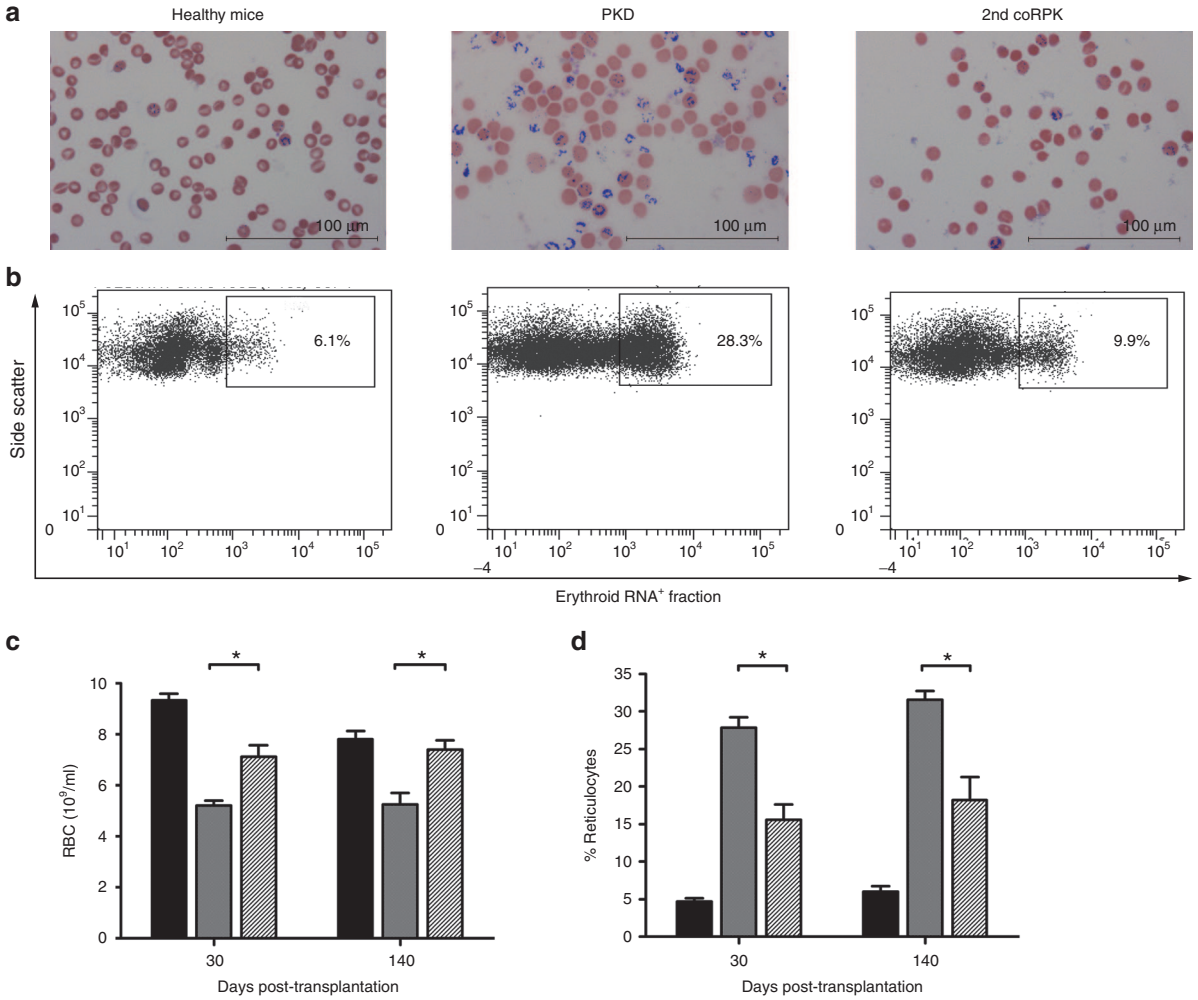

Figure 2 Pyruvate kinase deficiency phenotype correction in secondary transplanted mice. (**a**) Brilliant Cresyl blue staining of blood smears from nontransplanted mice and secondary (2nd coRPK) recipients to identify reticulocyte population (in blue). (**b**) Flow cytometry analysis of reticulocyte levels in peripheral blood. (**c**) RBCs and (**d**) reticulocyte percentage in secondary transplanted mice expressing the coRPK transgene (scratched bar, *n* = 4), in healthy mice (black bar, *n* = 3) and in anemic control mice (gray bar, *n* = 3). Data are represented the average ± standard error of the mean and were analyzed by nonparametric two-tailed Mann-Whitney test.

corrected mice, reducing the RBC accumulations and normalizing spleen histological structure and size (Figure 4). Additionally, histological studies revealed the total absence of iron deposits in the liver of genetically corrected mice, whereas PKD mice either from the nontransplanted group or the group transplanted with HSCs transduced with the EGFP-carrying vector displayed an intense iron overload due to the continuous hemolytic process (Figure 4c). Overall, the transplant of genetically corrected HSCs in PKD mice restored the normal status of the erythropoiesis and all the secondary effects caused by the hemolytic anemia.

PGK-coRPK LV-derived expression restores the glycolysis pathway in RBCs without modifying the WBC metabolic balance

Next, we performed an extensive metabolomic analysis of all transplanted and control mice to study the functional correction of RPK enzymatic activity. Following an untargeted profiling strategy, we observed significant changes of glycolytic intermediates in RBCs among the different groups, identifying three broad clusters of metabolite patterns with distinct trends (Figure 5a). RBCs from coRPK-expressing mice showed an increase of metabolites from cluster 1 similar to healthy controls but different from transplanted mice carrying the EGFP transgene. Likewise, cluster 3 reflected a reduced metabolite trend in genetically corrected mice similar to wild-type mice and different from EGFP-expressing mice. Nevertheless, cluster 2 from assay 1 showed no differences of metabolite profile between transplanted mouse groups (EGFP and coRPK expressing mice) (Figure 5a). The untargeted metabolic profiling also showed that the genetic modification was capable of modifying some important glycolytic intermediates, achieving an increase in ATP (Figure 5b), pyruvate (Figure 5d) and decrease in ADP levels (Figure 5c) in erythrocytes isolated from mice transplanted with PGK-coRPK LV-transduced HSCs. Considering these metabolic trends, we then analyzed other metabolites located closer to the PK-catalyzed reaction using a targeted profiling approach. Levels of the direct PK substrate phosphoenolpyruvate (Figure 5e) and the 3-phosphoglycerate (3-PG) (Figure 5f), located upstream of the PK-catalyzed reaction, approached to

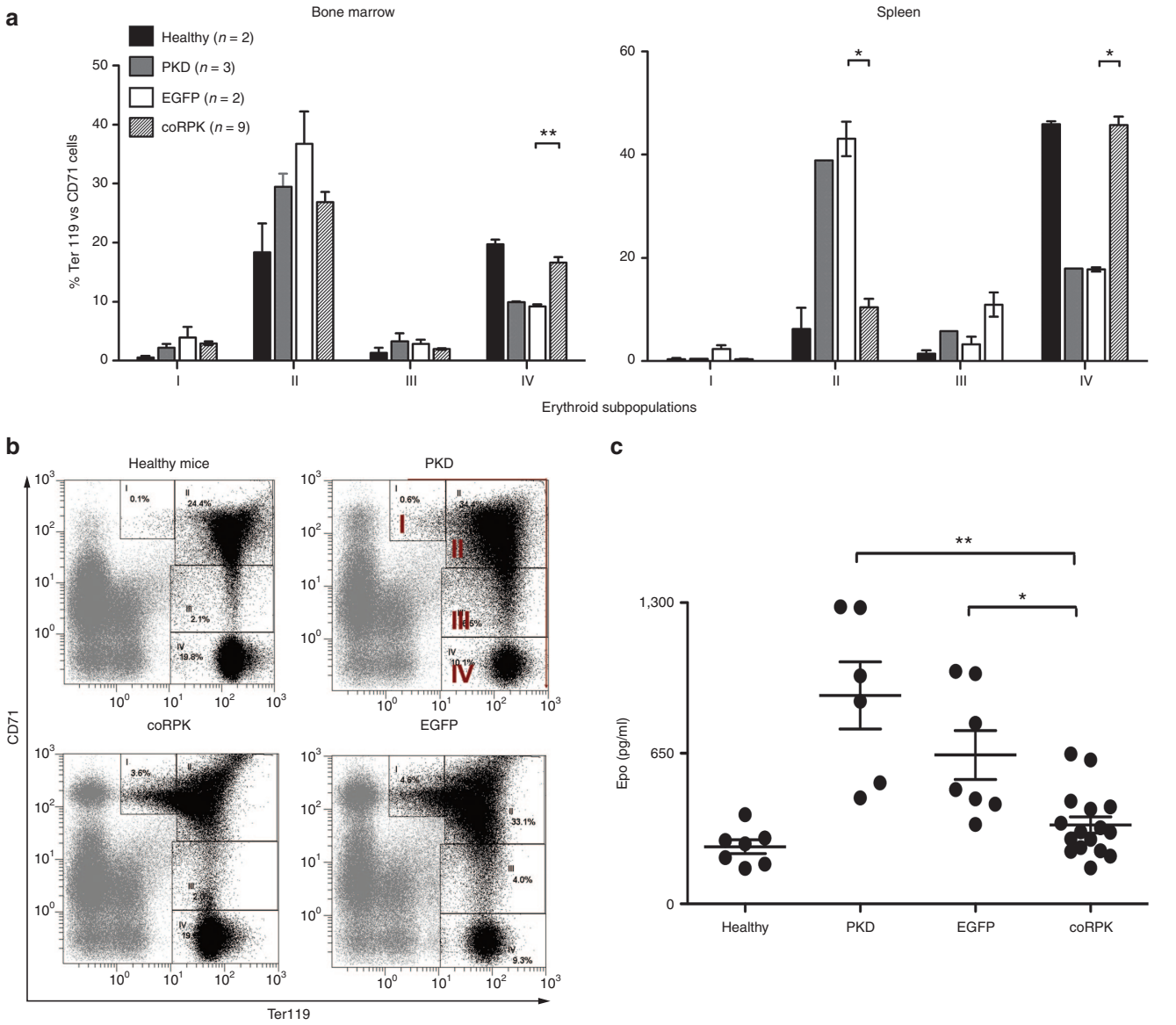

Figure 3 Normalization of the erythroid differentiation pattern in genetically corrected mice. (**a**) Percentages of the different erythroid subpopulation in bone marrow and spleen at 140 days after transplant. (**b**) Representative dot plots of the flow cytometry strategy used. The expression intensity of the CD71 and Ter119 markers allows for identifying four erythroid subpopulations: population I: early proerythroblasts (Ter119^{med} CD71^{high}), population II: basophilic erythroblasts (Ter119^{high} CD71^{high}), population III: late basophilic and polychromatophilic erythroblasts (Ter119^{high} CD71^{med}), and population IV: orthochromatophilic erythroblasts, reticulocytes and mature erythroid cells (Ter119^{high} CD71^{low}). (**c**) Plasma Epo levels measured by enzyme-linked immunosorbent assay (ELISA) in nontransplanted and transplanted mice. Dots represent values of individual mice. Lines represent average ± standard error of the mean and were analyzed by nonparametric Kruskal-Wallis test. Healthy, nontransplanted control mice; PKD, nontransplanted PKD mice; EGFP, PKD mice expressing the EGFP transgene; coRPK, PKD mice expressing the therapeutic transgene. PKD, pyruvate kinase deficiency.

that of healthy control mice. Deficient erythrocytes expressing the coRPK transgene also produced an increase of D-lactate (**Figure 5g**), the final product of the anaerobic glycolysis, when compared to PKD and EGFP expressing mice. To test whether the compensation in the glycolytic metabolites was a result of the normalization in PK activity in mature erythrocytes, we measured the activity of this enzyme and normalized it in relation to the Hexokinase (HK) activity in order to avoid the influence of high amounts of reticulocytes in the deficient animals. RBCs were purified through a cellulose column to prevent leukocyte PK activity contamination. A complete compensation of PK activity was observed in the animals expressing the coRPK that reached ratios similar to those obtained from wild-type healthy animals and from a normal healthy blood donor volunteer (**Supplementary Figure S5**).

Principal component analysis showed that metabolite pattern of RBCs was different depending on the group and markedly different to WBC profile (**Figure 6a**). On the contrary, WBC subgroups clustered together with very little difference among groups, indicating no changes in the metabolic balance of leukocytes when expressing the ectopic coRPK (**Figure 6a**). Additionally, specific metabolite changes observed in the RBC untargeted profiling were not present in WBCs (**Figure 6b–d**).

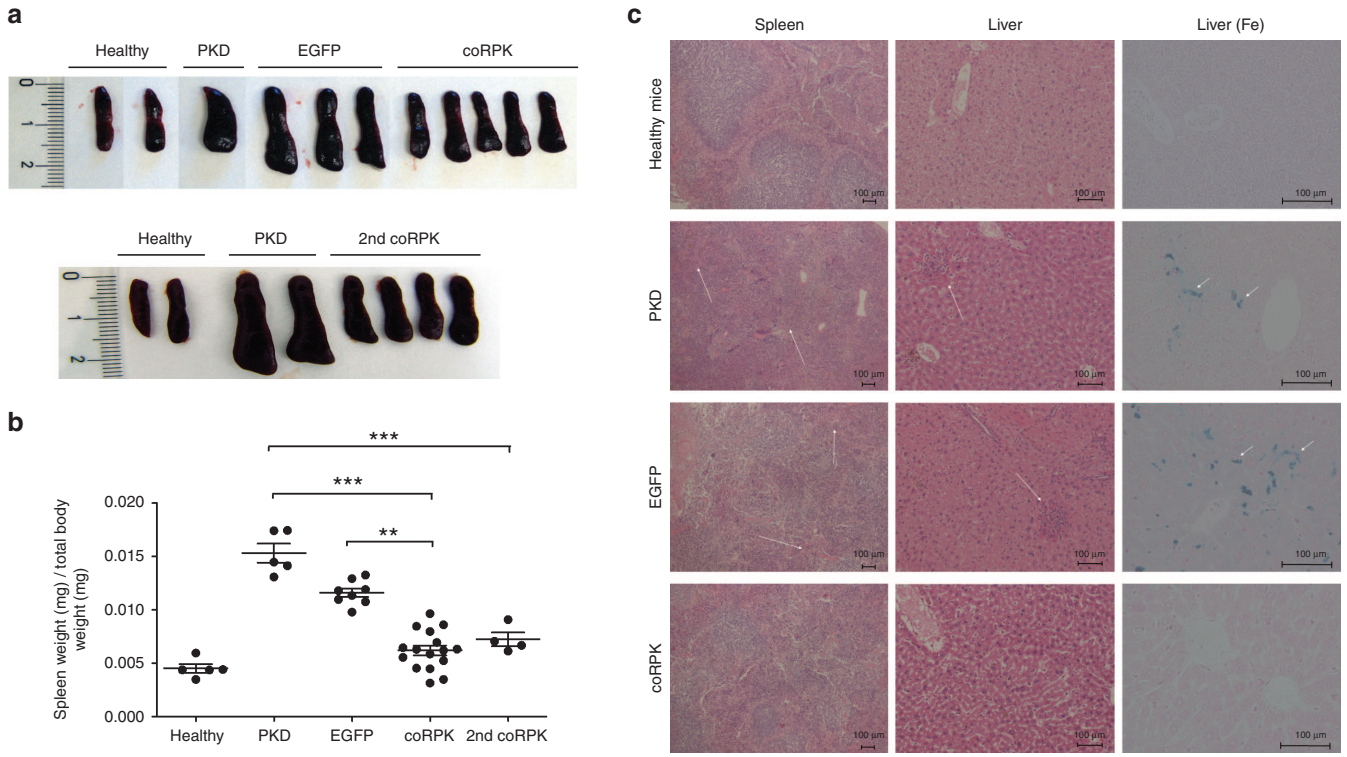

Figure 4 Reversion of splenomegaly and organ pathology in genetically corrected mice at 140 days post-transplantation. (**a**) Pictures of representative spleens and (**b**) ratio of spleen weight to total body weight from primary and secondary transplanted pyruvate kinase deficiency (PKD) mice. Dots represent values of individual mice. Lines represent average ± standard error of the mean per group. Data were analyzed by nonparametric Kruskal-Wallis test. (**c**) Histological study of spleen and liver from primary transplanted PKD mice. First and second column show the representative histology sections of spleen and liver stained with hematoxylin-eosin and photographed using a 4 and 10× objective, respectively, in a light microscope. Arrows point to erythroid cell clusters indicative of extramedullary erythropoiesis. Third column shows Prussian blue staining (Fe) of liver sections to detect iron deposits indicated by arrowheads. Photographs were taken using a 20× objective. Group legends as in Figure 3. 2nd coRPK, secondary recipients.

PGK-coRPK LV-transduced cells render polyclonal hematopoietic reconstitution without evidence of vector genotoxicity

Integration profile of LVs carrying either the coRPK or the EGFP transgene was analyzed in transplanted mice. Resulting from the genome-wide integration profile of LVs, each insertion creates a unique genetic mark that can be used to track the clonal behavior in individual transduced cells. Genomic DNA (gDNA) was obtained from WBCs and from BM cells and from primary and secondary transplanted mice, as well as from transduced cell pools before transplant (Lin$^-$ cells). Linear amplification-mediated polymerase chain reaction (LAM-PCR) (**Supplementary Figures S6 and S7**) was used to amplify vector/genome junctions, and to identify vector insertion sites (ISs). PCR products were sequenced by MiSeq Illumina platform and the obtained sequences were mapped onto the mouse genome by bioinformatics pipeline and filtered for collisions as described in **Supplementary Methods** (**Supplementary Figure S8**). Overall, we mapped 5,173,892 sequencing reads on the transplanted mouse genome, resulting in 2,220 unique vector integration sites. The genomic distribution of ISs from two independent experiments matched the previously reported LV preference for integration within transcriptional units (particularly within the first 50 Kb downstream of the transcription start site) (**Supplementary Figure S9a**), showing no skewing toward any particular chromosome in the mouse genome (**Supplementary Figure S9b**).

Safety of the PGK-coRPK LV-based gene therapy was studied by clonal abundance estimations, calculating the percentage of sequence count for each IS (a clonal mark) with respect to the total number of sequences of the dataset. Dot plots and heat map representations of the relative abundance of each IS retrieved for each mouse (**Figure 7**; **Supplementary Figures S10 and S11**) showed strong fluctuations in clonal composition of the different mice and of *in vitro* cultured Lin$^-$ cells. Also, it was possible to appreciate that for several samples, a small number of integrations contributed to a large amount of sequence reads (**Figure 7** and **Supplementary Figure S10**), revealing a polyclonal pattern of repopulation of transduced HSCs. In addition, tracked shared integration between primary mice carrying the therapeutic PGK-coRPK LV and subsequently transplanted secondary mice showed no strong sharing of integrations between the groups, confirming the absence of clonal dominance (**Supplementary Figure S10**).

To determine whether hallmarks of insertional mutagenesis were present in transplanted mice, we assessed the occurrence of common insertion sites (CIS) similar to currently ongoing LV-mediated clinical trials.[10,11,13,14,27] CIS are insertional hotspots that may result from integration bias at the time of transduction or *in vivo* selection of clones harboring vector integrations that

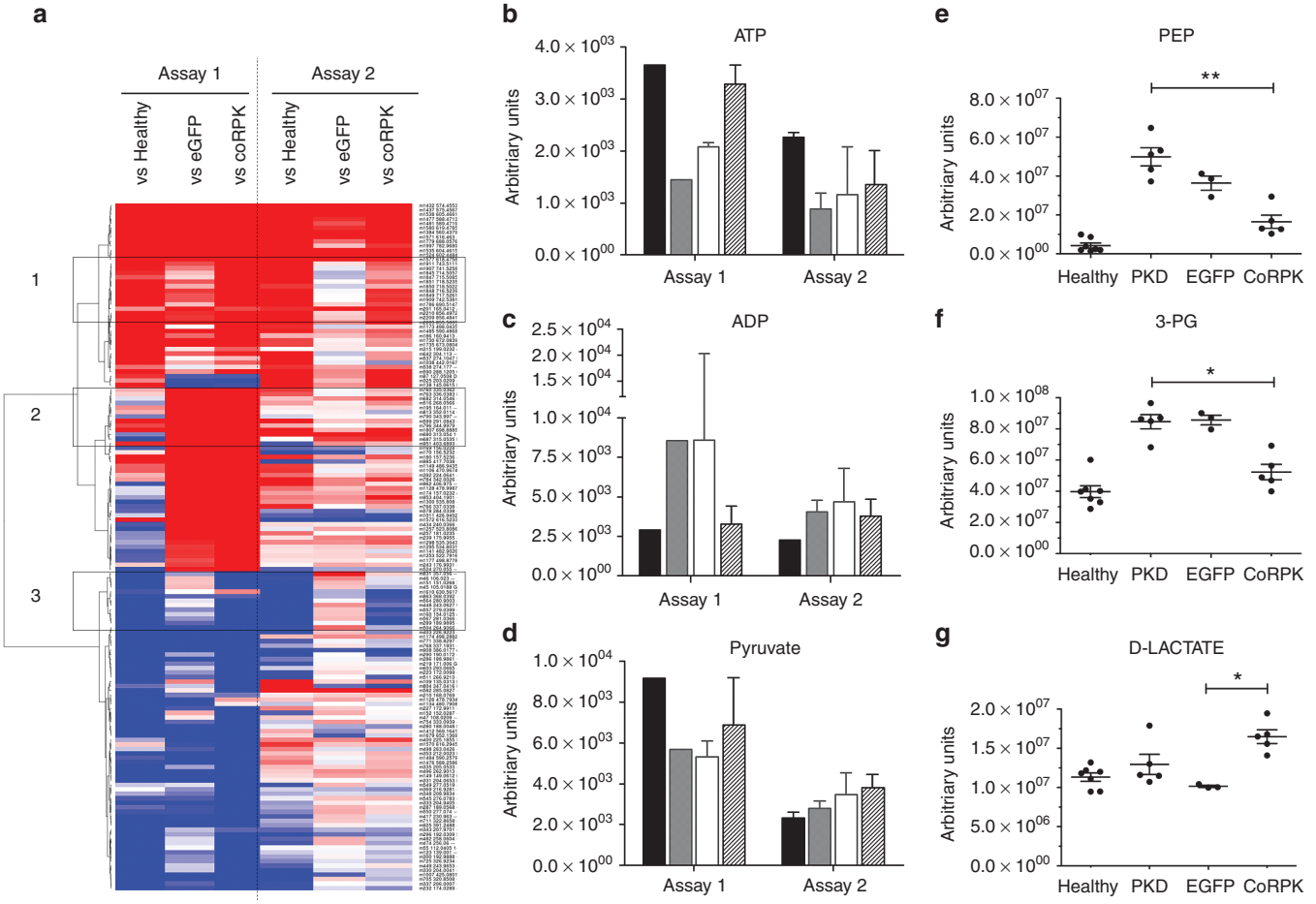

Figure 5 Metabolic profiling in RBC samples from mice transplanted with genetically modified cells. Analysis of significant metabolic profile changes in healthy and transplanted mice by comparison to pyruvate kinase deficiency (PKD) animals in two independent experiments. **(a)** Complete RBC heat map obtained by untargeted profiling, where higher and lower metabolite levels are represented in red and blue respectively. Metabolites listed have at least one comparison that is significant using the following criteria: absolute fold change >1.5; minimal signal >2,000; adjusted *P* value < 0.01. Black boxes highlight cluster of metabolite changes with distinct profile among the groups. (**b–d**) ATP, ADP, and pyruvate levels in RBCs, respectively, measured by untargeted profiling by comparison to PKD mice at 140 days after transplant. Assay 1: Healthy mice (black bars) *n* = 1, PKD (gray bars) *n* = 1, hPGK-EGFP (white bars) *n* = 2, hPGK-coRPK (scratched bars) *n* = 3. Assay 2: Healthy mice *n* = 2, PKD *n* = 2, hPGK-EGFP *n* = 6, hPGK-coRPK *n* = 10. (**e–g**) RBC targeted metabolic profiling of a selected number of metabolites involved in the glycolytic pathway (phosphoenolpyruvate, 3-phosphoglyceric acid and D-lactic acid, respectively) at 280 days post-transplantation. Dots represent values of individual mice. Lines represent average ± standard error of the mean and were analyzed by nonparametric Kruskal-Wallis test. Assay 2: Healthy mice *n* = 7, PKD *n* = 5, hPGK-EGFP *n* = 3, hPGK-coRPK *n* = 5.

confer growth advantage.[22,28–31] CIS were identified using an algorithm based on Abel and cols[32] and the Grubbs test for outliers,[27] finding no CIS and thus no alarming signs of genotoxicity by this readout. Moreover, gene ontology analysis revealed no skewing toward gene classes involved in cancer, cell proliferation or regulation of apoptosis in any of the integration datasets sorted by tissue-distribution, time point or abundance of repopulating hematopoietic cell clones (**Supplementary Figure S12**). These results suggest neutrality of vector integration and demonstrate the safety of the PGK-coRPK LV in a preclinical setting.

DISCUSSION

Genetic correction of erythroid metabolic diseases such as Glucose-6-phosphate dehydrogenase (G6PD) deficiency and PKD has yielded promising results in animal models,[18,33] but the insertional oncogenic risk observed in the first gene therapy trials using γ-RV vectors[21,24] made necessary to develop safer and more sophisticated tools to provide gene therapy a valid therapeutic option for PKD. Here, we show preclinical evidence that the PGK-coRPK LV efficiently rescues PKD pathology upon genetic correction and transplantation of HSCs in deficient mice. Furthermore, the safety-optimized design of the therapeutic vector leads to a safe genetic correction without modifying metabolic energy balance in leukocytes or causing side effects derived from vector integration.

Based on the efficacy and safety properties of LVs currently used in HSC gene therapy,[11–14] we designed a self-inactivating LV carrying a codon-optimized version of the human wild-type *PKLR* gene (coRPK) that led to normal levels of all hematological variables (RBCs, hemoglobin levels, hematocrit index, mean corpuscular volume, and mean corpuscular hemoglobin) and rapidly restored RPK to normal functioning in erythroid cells providing normal reticulocyte and inmature erythroide cell levels in gene therapy treated mice close to healthy controls. The PGK-coRPK LV treatment also led to an increased RBC survival, proportional

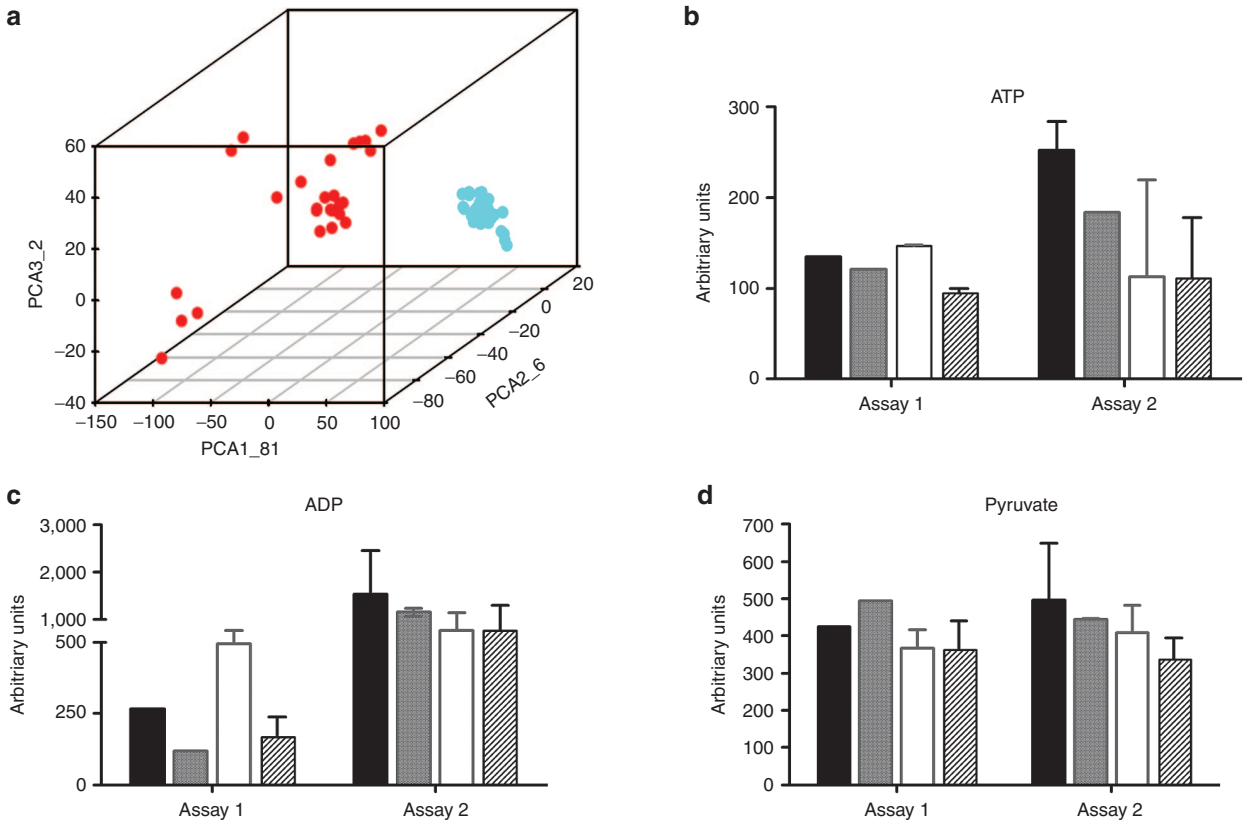

Figure 6 Untargeted metabolic profiling in WBC samples from mice transplanted with genetically modified cells. (**a**) Principal component analysis of untargeted metabolite profile in RBCs (red dots) and WBCs (blue dots) in control and transplanted mice. (**b–d**) ATP, ADP, and pyruvate levels, respectively, in WBCs by comparison to pyruvate kinase deficiency (PKD) mice. Assay 1: healthy mice (black bars) $n = 1$, PKD (gray bars) $n = 1$, hPGK-EGFP (white bars) $n = 2$, hPGK-coRPK (scratched bars) $n = 3$. Assay 2: healthy mice $n = 2$, PKD $n = 2$, hPGK-EGFP $n = 6$, hPGK-coRPK $n = 10$. Data represent the average ± standard error of the mean per group and were analyzed by nonparametric Kruskal-Wallis test.

to the level of donor chimerism detected in genetically corrected mice.

In PKD pathology, the hemolytic process triggers the mechanism of compensatory erythropoiesis to mitigate the quick loss of damaged RBCs, but this rapid development of new erythrocytes turns out that it is ineffective leading to an increased apoptosis in the erythroid compartment.[34] Some of the proposed explanations are membrane rigidity[35] and metabolic block caused by glycolytic intermediates accumulation[6,36] and the potential impairment of oxidative stress response[36] as a consequence of ATP depletion. The genetic correction with the PGK-coRPK LV however, normalizes the erythroid differentiation pattern in BM and spleen because the vector-derived RPK expression leads to an improved metabolic status of the basophilic erythroblasts, the stage in which RPK expression starts to be predominant[37] and allows the proper differentiation into the next stage of erythroid maturation. The correction of ineffective erythropoiesis in transplanted mice suggests that the PGK promoter drives a stable and robust expression of the coRPK transgene, able to resist the epigenetic changes that erythroid progenitor cells undergo upon differentiation into mature RBCs. On top of that, the characteristic splenomegaly present both in patients[6] and in PKD mice[38] was also reverted after genetic correction even with a moderate percentage of transduced cells (62% of CFU progenitors carrying the integrated provirus). Reduction of extramedullary erythropoiesis and iron overload in the spleen and liver of transplanted mice, significant reduction of plasma Epo levels and spleen CFU content normalization in coRPK-expressing mice demonstrates an almost complete recovery of the PKD pathology to the normal stage. Nevertheless, EGFP-expressing mice show a slight reduction of spleen weight that may be related to the effects associated to the hematopoietic transplantation procedure, such as the proliferative stage of the hematopoietic progenitors after the transplant.

The PKD phenotype correction provided by the developed therapeutic vector was further confirmed by metabolomic analysis, demonstrating that the metabolite profile of the corrected erythrocytes is similar to the healthy one and different from PKD mice and from PKD mice transplanted with cells transduced with the EGFP expressing vector. Although untargeted metabolite profiling shows cluster similarities between groups of transplanted mice (cluster 2, eGFP and coRPK), these similarities could be attributed to the BM transplant procedure that would affect both groups, and no matter the PKD phenotype was corrected. Clusters 1 and 3 reveal an increase and a decrease metabolite trend, respectively, in genetically corrected mice and in healthy controls that is different from mice carrying the EGFP transgene. This includes an increase of pyruvate and ATP levels and a decrease of ADP in RBCs that, in spite of not being significant, probably because of the bulk metabolite analysis, suggests the correction of the glycolytic pathway upon genetic correction. Targeted metabolomic analysis showed a significant

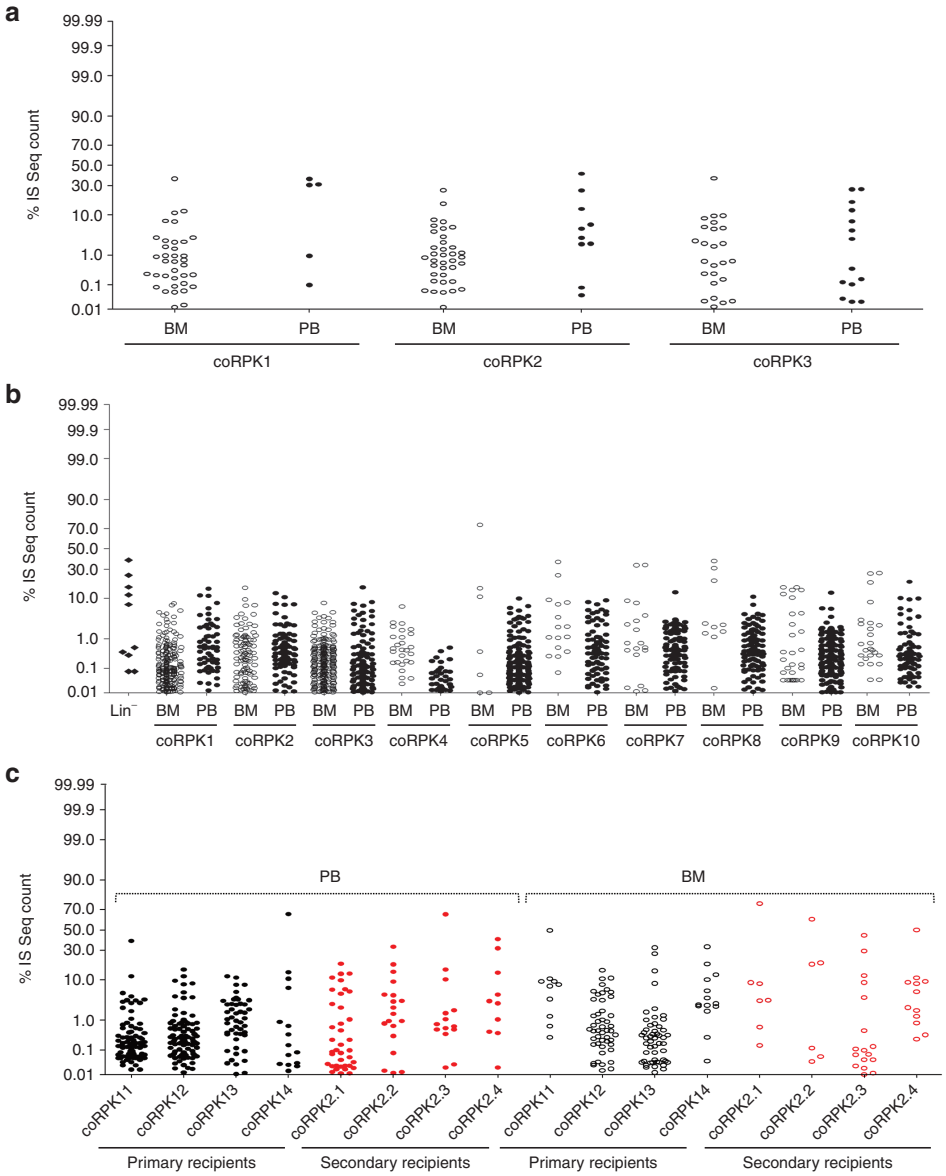

Figure 7 Clonal abundance analysis of coRPK-LV-transduced cells. Dots plot representation of clonal abundance of pooled integrations in each mouse from assays 1 (**a**) and 2 (**b,c**). The relative percentage (y-axis) for each integration site is relative to the total number of sequences reads obtained in each dataset. BM, bone marrow; IS, integration site; PB, peripheral blood; coRPK1-14, mice transplanted with hematopoietic cells transduced with the therapeutic vector. coRPK 2.1-2.4, secondary recipients transplanted with BM cells from coRPK 11-14 primary mice.

normalization not only of relevant metabolites located upstream of the RPK-catalyzed reaction (phosphoenolpyruvate, 3-PG, and D-lactate), but also intermediates of pentose phosphate pathway (not shown), pointing to a normal function of glycolysis pathway when RBCs express functional RPKs. Moreover, the PK enzyme activity, showed as the ratio PK/HK to compensate the differences in the amount of reticulocytes in healthy and diseased animals, clearly points toward the complete recovery of the PK function in the corrected erythrocytes. Interestingly, the ratio obtained was also similar to the one obtained in blood from a normal healthy volunteer, suggesting physiological levels of vector-derived PK activity and further demonstrating the capacity of the vector to compensate PKD. Remarkably, WBCs analyzed in parallel showed no alterations of the metabolic balance in leukocytes when RPK is ectopically expressed under the control of a ubiquitous promoter such as PGK, ruling out a leukocyte metabolic advantage as a possible safety concern and reinforcing the therapeutic potential of the PGK-coRPK LV.

The multi-lineage reconstitution and the absence of any leukemic event or clonal expansion in secondary recipients demonstrate the long-term stability and safety of the PGK-coRPK LV-based protocol that was further confirmed through the analysis of vector integration sites, an approach that is being increasingly used to predict the risk of insertional oncogenesis in HSC gene therapy clinical trials and in preclinical studies.[10,11,13,14,22,27,28,30,31] The analysis relative to the abundance of specific cell clones carrying the integrated vector shows a limited number of vector-marked clones repopulating the hematopoiesis in genetically corrected mice. Despite this polyclonal reconstitution pattern, CIS analysis did not

show any alarming sign of genotoxicity. Also, highly represented clones found at a certain time-point after transplant in some mice were reduced at longer times or absent in BM, indicating a high turnover and no clonal dominance of PGK-coRPK LV-corrected HSCs. Importantly, secondary transplanted mice showed integration sites found in primary recipients indicating that stem cells were marked, and in new integration sites not previously detected in primary recipients, pointing to the healthy clonal dynamics of hematopoiesis after genetic correction. These results suggest that the polyclonal nature of reconstitution observed is likely a consequence of the biology of hematopoietic reconstitution in mice.[39] In addition, gene ontology analysis revealed no skewing toward gene classes involved in cancer, cell proliferation or regulation of apoptosis.[40] Interestingly, the gene ontology study also showed that genes involved in catabolism were the ones most targeted by vector integration. This trend is different to that observed in other studies directed to other gene deficiencies,[41,42] and suggests that the viral integration pattern could be biased by the genetic deficiency of the recipient animals. Overall, the analysis of the vector integration pattern emphasizes the safety properties of the PGK-coRPK LV that provides PKD genetic correction with no signs of genotoxicity.

The development of gene therapy protocols for PKD is challenging and requires the precise balance between efficacy and safety. Firstly, the lack of selective advantage of corrected HSCs in erythroid metabolic deficiencies such as PKD[18–20] makes necessary the development of efficient vectors to ensure the expression of the transgene in mature affected RBCs and high levels of chimerism to ensure a high production of corrected erythrocytes. Secondly, high levels of wild-type RPK expression would be desirable to increase the expression of human monomers, increasing the probability of accumulating functional RPK tetramers, since the formation of heterotetramers between vector-derived functional copies of PK and endogenous nonfunctional monomers might reduce the efficacy of gene therapy for PKD. The PGK-coRPK LV leads to a complete phenotype correction when transduction levels fell to 62% with an estimated 1.02 transgene copies per cell, consistent with the VCN obtained in other preclinical studies, *i.e.*, β-thalassemia using a LV.[41] Nonetheless, pathological manifestations are usually observed in PKD patients when RPK activity falls below 25% of the normal activity,[43] and a similar level of corrected cells has been reported therapeutic in previous gene therapy protocols both in mouse[18] and dog models.[19] Hence, a phenotype correction may be expected even with lower levels of chimerism[18,19] and it is reasonable to expect a therapeutic benefit even if normal levels of RPK expression are not achieved after genetic correction. In this scenario, the single-gene PGK-coRPK LV design is essential and the use of the human PGK eukaryotic promoter, currently being used in a clinical trial,[14] provides transgene stable expression[44] and has been proven to be a weak transactivator[45]. Taken together, these have likely contributed to its therapeutic efficacy and safety, together with the optimization of the transgene sequence to increase expression[46] and the inclusion of the mutated Wpre sequence to increase mRNA stability.[47]

Our PGK-coRPK LV-based protocol would be able to correct the wide number of mutations described in PKD patients[1,2,4–6,48] including mutations in the regulatory sequences of the gene.[49,50] Also, considering that *PKLR* null mutations are rare,[6] the probability of developing an immunological response against the exogenous protein would be reduced. Even so, a patient-specific strategy based on the CRISPR/Cas9 correction of the endogenous locus would prevent the risk of insertional mutagenesis. This technology is currently being developed in our laboratory using $CD34^+$ HSCs from PKD patients with promising results, albeit with efficiencies very far from potentially applicable to the clinical setting yet. Overall, our findings demonstrate for the first time the feasibility of treating metabolic inherited erythroid disease through the genetic modification of HSCs using a safety-engineered LV vector.

MATERIALS AND METHODS

Animals. The AcB55 recombinant congenic mice (also recorded as PKD mice) carrying the 269T>A loss-of-function mutation in the *Pklr* gene, were used throughout.[26,51] AcB55 mice were obtained from Emerillon Therapeutics (Montreal, Quebec, Canada) and maintained at the Animal Facility Laboratory of CIEMAT (registration number ES280790000183) by inbreeding. C57BL/6 mice, and occasionally A/J mice, were used as healthy controls.

Lentiviral vectors production and transplantation of murine HSCs. LVs backbones were generated as shown in **Supplementary Figure S1a** and vectors stocks were produced as previously described.[52] Lineage negative cells (Lin^-) were obtained from the BM of 8–14-week-old male PKD mice, prestimulated with 100 ng/ml of recombinant human IL-11 (Peprotech EC, London, UK) and 100 ng/ml of recombinant murine stem cell factor (SCF) (R&D Systems, Minneapolis, MN) for 24 hours and then transduced with EGFP or coRPK carrying LVs in two cycles of transduction at multiplicities of infection (MOIs) of 1–10 vp/cell (**Supplementary Figure S1b**). Each transduction was carried out for 24 hours overnight. Approximately, 4×10^4 (assay 1) to 2×10^5 (assay 2 and 3) transduced Lin^- per mouse were intravenously injected into 8–14-week-old female PKD mice previously irradiated with a lethal dose of 9.5 Gy, split into two doses of 4.75 Gy 24 hours apart using a Philips MG324 X-ray instrument (Philips, Hamburg, Germany). Transplanted mice were monitored for 5 to 9 months and total BM was harvested at the end-point of the experiment to perform secondary transplants (4×10^6 cells/mouse).

Hematological variables and* in vivo *RBC survival. Mouse blood was collected from tail veins and analyzed in an automated blood cell analyzer (Abacus Junior vet, CMV Analitica, Spain). Reticulocyte percentage was determined in noncoagulated blood by staining with 0.5 μg/ml of Acridine Orange (Invitrogen Life Technologies, Grand Island, NY) and analyzed in an EPICS XL flow cytometer (Beckman Coulter Electronics, Hialeah, FL). Additionally, reticulocytes were identified in blood smears by Brilliant Cresyl Blue staining (Reagena, Toivala, Finland) and Giemsa counterstaining, and analyzed in a Leica Microsystems microscope. *In vivo* staining of RBCs was carried out following a previously published protocol of *in vivo* biotin staining.[38,53]

Structural and histological studies. Spleen and liver were studied following conventional histological methods (see **Supplementary Information**).

Colony forming cell (CFC) assays, erythroid differentiation, and plasma erythropoietin (EPO) levels. CFC assays were performed following manufacturer´s recommendations (Stem Cell Technologies, Vancouver, Canada). Erythroid differentiation was studied as described elsewhere[54] and Epo concentration was quantified using the Quantikine Mouse Epo immunoassay kit (MEP00B R&D Systems).

Provirus quantification and chimerism. Detection and quantification of integrated provirus per cell was accomplished by multiplex qPCR following a previously described strategy.[55] Additionally, colonies were singly picked to evaluate the VCN and the percentage of transduction. Chimerism levels were determined by detecting the presence of the Y chromosome as described elsewhere.[56]

Metabolomic studies. RBCs and WBCs were subjected to metabolomics studies.[57] RBCs were obtained from the whole blood after 2,500 rpm/10 minute centrifugation to remove the plasma and WBC interface. WBCs were obtained by erythrocyte lysis and centrifugation of PB. Pellets were stored at −80 °C. Metabolite extraction was carried out by adding 5 volumes of 70 °C 70% ethanol to one volume of cell pellet, and centrifugation at 3,000 rpm to pellet the precipitated protein. Thirty microliters of supernatant were transferred to a 96-well plate and dried under nitrogen. Samples were then resuspended in 30 µl of water to allow for metabolite profiling by mass spectrometry. Two approaches were used to collect metabolite profiles from the isolated blood components: (i) a targeted triple-quadruple-liquid chromatography mass spectrophotometry (LCMS) approach for the analysis of glycolytic and tricarboxylic acid cycle components, and (ii) an untargeted direct injection approach coupled to a high-mass-resolution Q-ToF. The targeted approach allowed for direct analysis of upstream/downstream metabolites from the pyruvate kinase enzyme, while the untargeted approach allowed for unbiased analysis of distal metabolic pathways.

General strategy for integration site analysis. The integration site analysis was performed according to the flowchart shown in **Supplementary Figure S8** that includes four main macro-activities going from "wet" sample processing to bioinformatics:

1. Wet lab procedures: LAM-PCRs and next-generation sequencing.
2. Next-generation sequencing data processing: acquiring as input sequencing reads from next-generation sequencing platforms and getting as output the list of integration sites.
3. Data quality processing: performing three sequential activities to improve data quality. Each activity generates the input for distinct processes in step 4.
4. IS-driven biological analysis: performing inferences on safety and efficacy of gene therapy.

See also extended version **Supplementary Text** for further details.

Abundance analysis. Clonality assessment was computed from the matrix files cleaned by contaminations (also called collisions). We used the three groups of mice independently (coRPK assay 1, EGFP assay 2, and coRPK assay 2. See **Supplementary Information**). For each group, the abundance value was obtained as the percentage for each IS of the sequence reads over the total reads of the group (**Figure 7** and **Supplementary Figure S11**). All values were obtained using Excel and then plotted the results using Prism. Excel files with the abundance representation as heat map are also available (**Supplementary Figure S10**).

Statistical analysis. Data from all experiments were represented as the average ± standard error of the mean. Two different nonparametric statistical tests were applied depending on the number of groups with no assumption of normal distribution of the data. When three or more experimental groups were compared, we used the Kruskal-Wallis test (*$P < 0.05$; **$P < 0.01$; ***$P < 0.001$), whereas two-tailed Mann-Whitney test was applied when only two groups were compared. RBC half-life studies were analyzed by two-way analysis of variance test (*$P < 0.05$; **$P < 0.01$; ***$P < 0.001$). Comparisons were carried out between transplanted mice and PKD littermates, and all statistical analyses were performed using GraphPad Prism software, version 5.0a (GraphPad Software, San Diego, CA).

Study approval. All experimental procedures were carried out according to European and Spanish laws and regulations (European convention ETS 1 2 3, regarding the use and protection of vertebrate mammals used in experimentation and other scientific purposes and Spanish Law 32/2007, R.D. 1201/2005 and RD 53/2013 regarding the protection and use of animals in scientific research). Procedures involving Genetically Modified Organism were approved by Spanish Biohazard Commission (Registration Number A/ES/04/I-04).

SUPPLEMENTARY MATERIAL

Table S1. Hematological variables recorded 140 days post-transplantation in peripheral blood.
Table S2. Relevant molecular parameters in mice transplanted with genetically modified cells.
Figure S1. Experiment design.
Figure S2. Multi-lineage hematopoietic reconstitution in secondary transplanted mice.
Figure S3. Quantification of proviral integrations.
Figure S4. Hematopoietic progenitor assays in control mice and transplanted mice with transduced cells
Figure S5. Pyruvate Kinase and Hexokinase activity in mice transplanted with transduced cells.
Figure S6. Gel image of LAM-PCR products generated with Tsp509I enzyme for samples harvested from all mice at different time points and tissues as Fig. S8 shows.
Figure S7. Gel image of LAM-PCR products generated with HpyCH4IV5 enzyme for samples harvested from all mice at different time points and tissues as Fig. S8 shows.
Figure S8. General scheme of the analysis of integration site mapping performed in mice transplanted with genetically modified hematopoietic progenitors.
Figure S9. Distribution of LV integrations along the genome of transplanted mice.
Figure S10. Tracked shared integrations between primary and secondary recipient mice carrying the therapeutic PGK-coRPK LV vector.
Figure S11. Clonal abundance analysis of EGFP-LV transduced cells.
Figure S12. LV genomic integration profile.
Supplementary Methods.
Supplementary Information.
Supplementary Text.

ACKNOWLEDGMENTS

The authors would like to thank Aurora de la Cal and Sergio Losada for their collaboration in the administrative work; Jesús Martínez and Edilia de Almeida for their careful maintenance of the animals, and Norman Feltz for reading and correcting the manuscript for style and grammar. This work was supported by the following grants: Dirección General de Investigación de la Comunidad de Madrid (CellCAM; Ref S2010/BMD-2420), Fondo de Investigaciones Sanitarias, Instituto de Salud Carlos III (RETICS-RD12/0019/0023) and MINECO (SAF2014-54885-R and SAF2012-31142). The authors declare no conflict of interest.

REFERENCES

1. Zanella, A, Bianchi, P and Fermo, E (2007). Pyruvate kinase deficiency. *Haematologica* **92**: 721–723.
2. Pissard, S, Max-Audit, I, Skopinski, L, Vasson, A, Vivien, P, Bimet, C *et al.* (2006). Pyruvate kinase deficiency in France: a 3-year study reveals 27 new mutations. *Br J Haematol* **133**: 683–689.
3. Gilsanz, F, Vega, MA, Gómez-Castillo, E, Ruiz-Balda, JA and Omeñaca, F (1993). Fetal anaemia due to pyruvate kinase deficiency. *Arch Dis Child* **69**(5 Spec No): 523–524.
4. Beutler, E and Gelbart, T (2000). Estimating the prevalence of pyruvate kinase deficiency from the gene frequency in the general white population. *Blood* **95**: 3585–3588.
5. Tanphaichitr, VS, Suvatte, V, Issaragrisil, S, Mahasandana, C, Veerakul, G, Chongkolwatana, V *et al.* (2000). Successful bone marrow transplantation in a child with red blood cell pyruvate kinase deficiency. *Bone Marrow Transplant* **26**: 689–690.
6. Zanella, A, Fermo, E, Bianchi, P and Valentini, G (2005). Red cell pyruvate kinase deficiency: molecular and clinical aspects. *Br J Haematol* **130**: 11–25.
7. Hilgard, P and Gerken, G (2005). Liver cirrhosis as a consequence of iron overload caused by hereditary nonspherocytic hemolytic anemia. *World J Gastroenterol* **11**: 1241–1244.
8. Kanno, H, Fujii, H and Miwa, S (1992). Structural analysis of human pyruvate kinase L-gene and identification of the promoter activity in erythroid cells. *Biochem Biophys Res Commun* **188**: 516–523.
9. Noguchi, T, Yamada, K, Inoue, H, Matsuda, T and Tanaka, T (1987). The L- and R-type isozymes of rat pyruvate kinase are produced from a single gene by use of different promoters. *J Biol Chem* **262**: 14366–14371.
10. Cartier, N, Hacein-Bey-Abina, S, Bartholomae, CC, Veres, G, Schmidt, M, Kutschera, I *et al.* (2009). Hematopoietic stem cell gene therapy with a lentiviral vector in X-linked adrenoleukodystrophy. *Science* **326**: 818–823.
11. Cavazzana-Calvo, M, Payen, E, Negre, O, Wang, G, Hehir, K, Fusil, F *et al.* (2010). Transfusion independence and HMGA2 activation after gene therapy of human β-thalassaemia. *Nature* **467**: 318–322.

12. Cartier, N, Hacein-Bey-Abina, S, Bartholomae, CC, Bougnères, P, Schmidt, M, Kalle, CV *et al.* (2012). Lentiviral hematopoietic cell gene therapy for X-linked adrenoleukodystrophy. *Methods Enzymol* **507**: 187–198.
13. Aiuti, A, Biasco, L, Scaramuzza, S, Ferrua, F, Cicalese, MP, Baricordi, C *et al.* (2013). Lentiviral hematopoietic stem cell gene therapy in patients with Wiskott-Aldrich syndrome. *Science* **341**: 1233151.
14. Biffi, A, Montini, E, Lorioli, L, Cesani, M, Fumagalli, F, Plati, T *et al.* (2013). Lentiviral hematopoietic stem cell gene therapy benefits metachromatic leukodystrophy. *Science* **341**: 1233158.
15. Pestina, TI, Hargrove, PW, Jay, D, Gray, JT, Boyd, KM and Persons, DA (2009). Correction of murine sickle cell disease using gamma-globin lentiviral vectors to mediate high-level expression of fetal hemoglobin. *Mol Ther* **17**: 245–252.
16. Breda, L, Casu, C, Gardenghi, S, Bianchi, N, Cartegni, L, Narla, M *et al.* (2012). Therapeutic hemoglobin levels after gene transfer in β-thalassemia mice and in hematopoietic cells of β-thalassemia and sickle cells disease patients. *PLoS One* **7**: e32345.
17. Tani, K, Yoshikubo, T, Ikebuchi, K, Takahashi, K, Tsuchiya, T, Takahashi, S *et al.* (1994). Retrovirus-mediated gene transfer of human pyruvate kinase (PK) cDNA into murine hematopoietic cells: implications for gene therapy of human PK deficiency. *Blood* **83**: 2305–2310.
18. Meza, NW, Alonso-Ferrero, ME, Navarro, S, Quintana-Bustamante, O, Valeri, A, Garcia-Gomez, M *et al.* (2009). Rescue of pyruvate kinase deficiency in mice by gene therapy using the human isoenzyme. *Mol Ther* **17**: 2000–2009.
19. Trobridge, GD, Beard, BC, Wu, RA, Ironside, C, Malik, P and Kiem, HP (2012). Stem cell selection *in vivo* using foamy vectors cures canine pyruvate kinase deficiency. *PLoS One* **7**: e45173.
20. Richard, RE, Weinreich, M, Chang, KH, Ieremia, J, Stevenson, MM and Blau, CA (2004). Modulating erythrocyte chimerism in a mouse model of pyruvate kinase deficiency. *Blood* **103**: 4432–4439.
21. Hacein-Bey-Abina, S, Garrigue, A, Wang, GP, Soulier, J, Lim, A, Morillon, E *et al.* (2008). Insertional oncogenesis in 4 patients after retrovirus-mediated gene therapy of SCID-X1. *J Clin Invest* **118**: 3132–3142.
22. Ott, MG, Schmidt, M, Schwarzwaelder, K, Stein, S, Siler, U, Koehl, U *et al.* (2006). Correction of X-linked chronic granulomatous disease by gene therapy, augmented by insertional activation of MDS1-EVI1, PRDM16 or SETBP1. *Nat Med* **12**: 401–409.
23. Howe, SJ, Mansour, MR, Schwarzwaelder, K, Bartholomae, C, Hubank, M, Kempski, H *et al.* (2008). Insertional mutagenesis combined with acquired somatic mutations causes leukemogenesis following gene therapy of SCID-X1 patients. *J Clin Invest* **118**: 3143–3150.
24. Stein, S, Ott, MG, Schultze-Strasser, S, Jauch, A, Burwinkel, B, Kinner, A *et al.* (2010). Genomic instability and myelodysplasia with monosomy 7 consequent to EVI1 activation after gene therapy for chronic granulomatous disease. *Nat Med* **16**: 198–204.
25. Braun, CJ, Boztug, K, Paruzynski, A, Witzel, M, Schwarzer, A, Rothe, M *et al.* (2014). Gene therapy for Wiskott-Aldrich syndrome–long-term efficacy and genotoxicity. *Sci Transl Med* **6**: 227ra33.
26. Min-Oo, G, Fortin, A, Tam, MF, Gros, P and Stevenson, MM (2004). Phenotypic expression of pyruvate kinase deficiency and protection against malaria in a mouse model. *Genes Immun* **5**: 168–175.
27. Biffi, A, Bartolomae, CC, Cesana, D, Cartier, N, Aubourg, P, Ranzani, M *et al.* (2011). Lentiviral vector common integration sites in preclinical models and a clinical trial reflect a benign integration bias and not oncogenic selection. *Blood* **117**: 5332–5339.
28. Schwarzwaelder, K, Howe, SJ, Schmidt, M, Brugman, MH, Deichmann, A, Glimm, H *et al.* (2007). Gammaretrovirus-mediated correction of SCID-X1 is associated with skewed vector integration site distribution in vivo. *J Clin Invest* **117**: 2241–2249.
29. Deichmann, A, Hacein-Bey-Abina, S, Schmidt, M, Garrigue, A, Brugman, MH, Hu, J *et al.* (2007). Vector integration is nonrandom and clustered and influences the fate of lymphopoiesis in SCID-X1 gene therapy. *J Clin Invest* **117**: 2225–2232.
30. Deichmann, A, Brugman, MH, Bartholomae, CC, Schwarzwaelder, K, Verstegen, MM, Howe, SJ *et al.* (2011). Insertion sites in engrafted cells cluster within a limited repertoire of genomic areas after gammaretroviral vector gene therapy. *Mol Ther* **19**: 2031–2039.
31. Hacein-Bey-Abina, S, Von Kalle, C, Schmidt, M, McCormack, MP, Wulffraat, N, Leboulch, P *et al.* (2003). LMO2-associated clonal T cell proliferation in two patients after gene therapy for SCID-X1. *Science* **302**: 415–419.
32. Abel, U, Deichmann, A, Nowrouzi, A, Gabriel, R, Bartholomae, CC, Glimm, H *et al.* (2011). Analyzing the number of common integration sites of viral vectors–new methods and computer programs. *PLoS One* **6**: e24247.
33. Rovira, A, De Angioletti, M, Camacho-Vanegas, O, Liu, D, Rosti, V, Gallardo, HF *et al.* (2000). Stable *in vivo* expression of glucose-6-phosphate dehydrogenase (G6PD) and rescue of G6PD deficiency in stem cells by gene transfer. *Blood* **96**: 4111–4117.
34. Aizawa, S, Harada, T, Kanbe, E, Tsuboi, I, Aisaki, K, Fujii, H *et al.* (2005). Ineffective erythropoiesis in mutant mice with deficient pyruvate kinase activity. *Exp Hematol* **33**: 1292–1298.
35. Miwa, S and Fujii, H (1985). Molecular aspects of erythroenzymopathies associated with hereditary hemolytic anemia. *Am J Hematol* **19**: 293–305.
36. Aisaki, K, Aizawa, S, Fujii, H, Kanno, J and Kanno, H (2007). Glycolytic inhibition by mutation of pyruvate kinase gene increases oxidative stress and causes apoptosis of a pyruvate kinase deficient cell line. *Exp Hematol* **35**: 1190–1200.
37. Nijhof, W, Wierenga, PK, Staal, GE and Jansen, G (1984). Changes in activities and isozyme patterns of glycolytic enzymes during erythroid differentiation *in vitro*. *Blood* **64**: 607–613.
38. Min-Oo, G, Tam, M, Stevenson, MM and Gros, P (2007). Pyruvate kinase deficiency: correlation between enzyme activity, extent of hemolytic anemia and protection against malaria in independent mouse mutants. *Blood Cells Mol Dis* **39**: 63–69.
39. Kustikova, OS, Schiedlmeier, B, Brugman, MH, Stahlhut, M, Bartels, S, Li, Z *et al.* (2009). Cell-intrinsic and vector-related properties cooperate to determine the incidence and consequences of insertional mutagenesis. *Mol Ther* **17**: 1537–1547.
40. Maruggi, G, Porcellini, S, Facchini, G, Perna, SK, Cattoglio, C, Sartori, D *et al.* (2009). Transcriptional enhancers induce insertional gene deregulation independently from the vector type and design. *Mol Ther* **17**: 851–856.
41. Ronen, K, Negre, O, Roth, S, Colomb, C, Malani, N, Denaro, M *et al.* (2011). Distribution of lentiviral vector integration sites in mice following therapeutic gene transfer to treat β-thalassemia. *Mol Ther* **19**: 1273–1286.
42. Molina-Estevez, FJ, Lozano, ML, Navarro, S, Torres, Y, Grabundzija, I, Ivics, Z *et al.* (2013). Brief report: impaired cell reprogramming in nonhomologous end joining deficient cells. *Stem Cells* **31**: 1726–1730.
43. Zanella, A, Bianchi, P, Fermo, E, Iurlo, A, Zappa, M, Vercellati, C *et al.* (2001). Molecular characterization of the PK-LR gene in sixteen pyruvate kinase-deficient patients. *Br J Haematol* **113**: 43–48.
44. Gerolami, R, Uch, R, Jordier, F, Chapel, S, Bagnis, C, Bréchot, C *et al.* (2000). Gene transfer to hepatocellular carcinoma: transduction efficacy and transgene expression kinetics by using retroviral and lentiviral vectors. *Cancer Gene Ther* **7**: 1286–1292.
45. Zychlinski, D, Schambach, A, Modlich, U, Maetzig, T, Meyer, J, Grassman, E *et al.* (2008). Physiological promoters reduce the genotoxic risk of integrating gene vectors. *Mol Ther* **16**: 718–725.
46. van Til, NP, de Boer, H, Mashamba, N, Wabik, A, Huston, M, Visser, TP *et al.* (2012). Correction of murine Rag2 severe combined immunodeficiency by lentiviral gene therapy using a codon-optimized RAG2 therapeutic transgene. *Mol Ther* **20**: 1968–1980.
47. Zanta-Boussif, MA, Charrier, S, Brice-Ouzet, A, Martin, S, Opolon, P, Thrasher, AJ *et al.* (2009). Validation of a mutated PRE sequence allowing high and sustained transgene expression while abrogating WHV-X protein synthesis: application to the gene therapy of WAS. *Gene Ther* **16**: 605–619.
48. Ferreira, P, Morais, L, Costa, R, Resende, C, Dias, CP, Araújo, F *et al.* (2000). Hydrops fetalis associated with erythrocyte pyruvate kinase deficiency. *Eur J Pediatr* **159**: 481–482.
49. Manco, L, Ribeiro, ML, Máximo, V, Almeida, H, Costa, A, Freitas, O *et al.* (2000). A new PKLR gene mutation in the R-type promoter region affects the gene transcription causing pyruvate kinase deficiency. *Br J Haematol* **110**: 993–997.
50. van Wijk, R, van Solinge, WW, Nerlov, C, Beutler, E, Gelbart, T, Rijksen, G *et al.* (2003). Disruption of a novel regulatory element in the erythroid-specific promoter of the human PKLR gene causes severe pyruvate kinase deficiency. *Blood* **101**: 1596–1602.
51. Min-Oo, G, Fortin, A, Tam, MF, Nantel, A, Stevenson, MM and Gros, P (2003). Pyruvate kinase deficiency in mice protects against malaria. *Nat Genet* **35**: 357–362.
52. Follenzi, A, Ailles, LE, Bakovic, S, Geuna, M and Naldini, L (2000). Gene transfer by lentiviral vectors is limited by nuclear translocation and rescued by HIV-1 pol sequences. *Nat Genet* **25**: 217–222.
53. Marinkovic, D, Zhang, X, Yalcin, S, Luciano, JP, Brugnara, C, Huber, T *et al.* (2007). Foxo3 is required for the regulation of oxidative stress in erythropoiesis. *J Clin Invest* **117**: 2133–2144.
54. Socolovsky, M, Nam, H, Fleming, MD, Haase, VH, Brugnara, C and Lodish, HF (2001). Ineffective erythropoiesis in Stat5a(-/-)5b(-/-) mice due to decreased survival of early erythroblasts. *Blood* **98**: 3261–3273.
55. Charrier, S, Ferrand, M, Zerbato, M, Précigout, G, Viornery, A, Bucher-Laurent, S *et al.* (2011). Quantification of lentiviral vector copy numbers in individual hematopoietic colony-forming cells shows vector dose-dependent effects on the frequency and level of transduction. *Gene Ther* **18**: 479–487.
56. Navarro, S, Meza, NW, Quintana-Bustamante, O, Casado, JA, Jacome, A, McAllister, K *et al.* (2006). Hematopoietic dysfunction in a mouse model for Fanconi anemia group D1. *Mol Ther* **14**: 525–535.
57. Fuhrer, T, Heer, D, Begemann, B and Zamboni, N (2011). High-throughput, accurate mass metabolome profiling of cellular extracts by flow injection-time-of-flight mass spectrometry. *Anal Chem* **83**: 7074–7080.